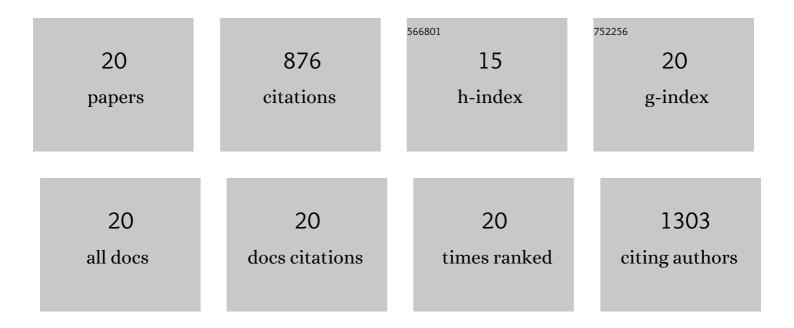
Isabel Dregely

List of Publications by Year in descending order

Source: https://exaly.com/author-pdf/9166723/publications.pdf Version: 2024-02-01



#	Article	IF	CITATIONS
1	Simultaneous magnetic resonance imaging of ventilation distribution and gas uptake in the human lung using hyperpolarized xenon-129. Proceedings of the National Academy of Sciences of the United States of America, 2010, 107, 21707-21712.	3.3	176
2	Hybrid PET/MR Imaging of the Heart: Potential, Initial Experiences, and Future Prospects. Journal of Nuclear Medicine, 2013, 54, 402-415.	2.8	144
3	Self-gated MRI motion modeling for respiratory motion compensation in integrated PET/MRI. Medical Image Analysis, 2015, 19, 110-120.	7.0	103
4	Hyperpolarized Xenonâ€129 gasâ€exchange imaging of lung microstructure: First case studies in subjects with obstructive lung disease. Journal of Magnetic Resonance Imaging, 2011, 33, 1052-1062.	1.9	85
5	Multipleâ€exchangeâ€time xenon polarization transfer contrast (MXTC) MRI: Initial results in animals and healthy volunteers. Magnetic Resonance in Medicine, 2012, 67, 943-953.	1.9	42
6	A 16-channel MR coil for simultaneous PET/MR imaging in breast cancer. European Radiology, 2015, 25, 1154-1161.	2.3	42
7	Freeâ€breathing liver fat quantification using a multiecho 3 <scp>D</scp> stackâ€ofâ€radial technique. Magnetic Resonance in Medicine, 2018, 79, 370-382.	1.9	40
8	Imaging biomarkers in oncology: Basics and application to MRI. Journal of Magnetic Resonance Imaging, 2018, 48, 13-26.	1.9	39
9	Self-gated Radial MRI for Respiratory Motion Compensation on Hybrid PET/MR Systems. Lecture Notes in Computer Science, 2013, 16, 17-24.	1.0	33
10	Singleâ€breath xenon polarization transfer contrast (SBâ€XTC): Implementation and initial results in healthy humans. Journal of Magnetic Resonance Imaging, 2013, 37, 457-470.	1.9	31
11	Convenient Synthesis of ⁶⁸ Ga‣abeled Gadolinium(III) Complexes: Towards Bimodal Responsive Probes for Functional Imaging with PET/MRI. Chemistry - A European Journal, 2013, 19, 12602-12606.	1.7	23
12	32â€channel phasedâ€array receive with asymmetric birdcage transmit coil for hyperpolarized xenonâ€129 lung imaging. Magnetic Resonance in Medicine, 2013, 70, 576-583.	1.9	22
13	Rapid quantitative T ₂ mapping of the prostate using threeâ€dimensional dual echo steady state MRI at 3T. Magnetic Resonance in Medicine, 2016, 76, 1720-1729.	1.9	22
14	Irreversible Electroporation: Defining the MRI Appearance of the Ablation Zone With Histopathologic Correlation in a Porcine Liver Model. American Journal of Roentgenology, 2017, 208, 1141-1146.	1.0	16
15	Accelerated 3D T ₂ mapping with dictionaryâ€based matching for prostate imaging. Magnetic Resonance in Medicine, 2019, 81, 1795-1805.	1.9	16
16	â€mapping with the transient phase of unbalanced steadyâ€state free precession. Magnetic Resonance in Medicine, 2013, 70, 1515-1523.	1.9	15
17	Accelerated 3D T ₂ wâ€maging of the prostate with 1â€millimeter isotropic resolution in less than 3 minutes. Magnetic Resonance in Medicine, 2019, 82, 721-731.	1.9	11
18	Optimization and evaluation of reference region variable flip angle (RRâ€VFA) and <i>T</i> ₁ Mapping in the Prostate at 3T. Journal of Magnetic Resonance Imaging, 2017, 45, 751-760.	1.9	8

#	Article	IF	CITATIONS
19	Observations With Simultaneous 18F-FDG PETÂand MR Imaging in Peripheral Artery Disease. JACC: Cardiovascular Imaging, 2017, 10, 709-711.	2.3	7
20	Distortionâ€free 3D diffusion imaging of the prostate using a multishot diffusionâ€prepared phaseâ€cycled acquisition and dictionary matching. Magnetic Resonance in Medicine, 2021, 85, 1441-1454.	1.9	1